Identification of Li$^+$ binding sites and the effect of Li$^+$ treatment on phospholipid composition in human neuroblastoma cells: A ^{7}Li and ^{31}P NMR study

Brian T. Layden[a], Abde M. Abukhdeir[a], Christopher Malarkey[a], Lisa A. Oriti[a], Wajeeh Salah[a], Claire Stigler[a], Carlos F.G.C. Geraldes[b], Duarte Mota de Freitas[a,*]

[a]Department of Chemistry, Loyola University Chicago, 6525 North Sheridan Road, Chicago, Illinois 60626, USA
[b]Department of Biochemistry, NMR Center and Center of Neurosciences and Cell Biology, University of Coimbra, P.O. Box 3126, 3001-401 Coimbra, Portugal

Abstract

Li$^+$ binding in subcellular fractions of human neuroblastoma SH-SY5Y cells was investigated using ^{7}Li NMR spin–lattice (T_1) and spin–spin (T_2) relaxation measurements, as the T_1/T_2 ratio is a sensitive parameter of Li$^+$ binding. The majority of Li$^+$ binding occurred in the plasma membrane, microsomes, and nuclear membrane fractions as demonstrated by the Li$^+$ binding constants and the values of the T_1/T_2 ratios, which were drastically larger than those observed in the cytosol, nuclei, and mitochondria. We also investigated by ^{31}P NMR spectroscopy the effects of chronic Li$^+$ treatment for 4–6 weeks on the phospholipid composition of the plasma membrane and the cell homogenate and found that the levels of phosphatidylinositol and phosphatidylserine were significantly increased and decreased, respectively, in both fractions. From these observations, we propose that Li$^+$ binding occurs predominantly to membrane domains, and that chronic Li$^+$ treatment alters the phospholipid composition at these membrane sites. These findings support those from clinical studies that have indicated that Li$^+$ treatment of bipolar patients results in irregularities in Li$^+$ binding and phospholipid metabolism. Implications of our observations on putative mechanisms of Li$^+$ action, including the cell membrane abnormality, the inositol depletion and the G-protein hypotheses, are discussed.
© 2005 Elsevier B.V. All rights reserved.

Keywords: Cell membrane; Cytosol; Lithium; Mitochondria; NMR; Phospholipid

1. Introduction

Lithium has been used for the treatment of bipolar disorder for more than 50 years without knowledge of its exact mechanism of action [1,2]. An improved under-standing of the molecular mechanism of the therapeutic action of Li$^+$ requires the investigation of the binding of Li$^+$ to the different subcellular fractions of the nerve cell and ascertaining the effect that chronic Li$^+$ treatment has on the Li$^+$ binding sites.

Previous studies on red blood cells (RBCs) used as a model cell line have addressed the question of where Li$^+$ binds in these cells [3–5]. In a ^{7}Li NMR relaxation study, the major Li$^+$ binding site in RBCs was determined to be the plasma membrane. In contrast, other RBC components such as hemoglobin, spectrin, 2,3-bisphosphoglycerate, and ATP were found to contribute only minimally toward Li$^+$ binding [5]. It was further determined that the inner leaflet of the

plasma membrane contributed more extensively to Li^+ binding than did the outer leaflet, due to the presence of more anionic phospholipids in the inner leaflet [5]. In a more recent study, it was demonstrated qualitatively that Li^+ was immobilized more in intact human neuroblastoma SH-SY5Y cells, a nerve cell model, than in intact RBCs [6]. Comparable Li^+ binding was, however, observed in suspensions of RBC and neuroblastoma plasma membranes [6]. This observation suggests that additional Li^+ binding sites accounted for the greater extent of Li^+ immobilization in neuroblastoma cells than in RBCs.

Membrane abnormalities have been suggested to occur in bipolar illness, based on observations of irregular Li^+-transport rates and phospholipid membrane composition in RBCs from Li^+-treated bipolar patients [7]. In particular, it has been found that rates of $Na^+–Li^+$ exchange in RBCs were significantly lower in Li^+-treated bipolar patients than in normal individuals [8,9]. Three weeks after discontinuation of Li^+ treatment, however, the $Na^+–Li^+$ exchange rates in these same patients returned to normal values, indicating an effect of Li^+ treatment [10,11]. Abnormal phospholipid composition has been observed in the RBC plasma membranes of Li^+-treated bipolar patients [9], which may explain that the decrease in Na^+/Li^+ transport rates results from altered interactions between metal ions and membrane proteins or lipids. Li^+ has been demonstrated to have varying binding affinities to different phospholipids isolated from RBC plasma membranes [12]. Specifically, Li^+ was shown to have the highest binding affinity to phosphatidyl serine (PS), followed by phosphatidyl inositol (PI). Sphingomyelin (SM), phosphatidyl ethanolamine (PE), β-acyl-γ-alkylphosphatidylcholine (PC_{AA}), and phosphatidyl choline (PC) were shown to have lower binding affinities to Li^+ than PS or PI. In contrast to the case of RBCs, the $Na^+–Ca^{2+}$ exchanger, and, to a smaller extent, the voltage-sensitive Na^+ channel and the $Na^+–Li^+$ exchanger, are the main Li^+ transport pathways in neuronal cells [6,13]. Unlike in RBCs, in neuronal cells from bipolar patients, however, the effects of Li^+ on $Na^+–Ca^{2+}$ exchange and on $Na^+–Li^+$ exchange, as well as on voltage-sensitive Na^+ transport rates, are unknown. Because the presumed site of Li^+ action in bipolar illness is neuronal tissue, the relationship between the membrane abnormality hypothesis in neuronal tissue and the pharmacologic action of Li^+ warrants further exploration.

To further our understanding of the applicability of this membrane abnormality hypothesis to neuronal cells, we examined two aspects of Li^+ action in human neuroblastoma SH-SY5Y cells: (1) the identification of major intracellular site(s) of Li^+ binding and (2) the effect of chronic Li^+ treatment on these binding sites. Using differential centrifugation techniques, we isolated subcellular fractions from human neuroblastoma SH-SY5Y cells. We used the ratio of measured ^7Li NMR spin–lattice (T_1) to spin–spin (T_2) relaxation rates, which is a sensitive measure of molecular mobility [3,4], to determine Li^+ binding characteristics in different subcellular fractions.

Because phospholipids are the major determinants of Li^+ binding to membrane fractions, phospholipid concentrations were determined by ^{31}P NMR spectroscopy in the cell homogenates and in the major Li^+ binding site, the plasma membrane, without prior Li^+ incubation and under chronic Li^+ incubation conditions (2.5 mM and 5.0 mM Li^+ over 4 to 6 weeks). We have also interpreted our observations on Li^+ binding sites and the effects of Li^+ incubation on the phospholipid composition of the plasma membrane in the SH-SY5Y nerve cell model in terms of putative mechanisms of lithium action.

2. Materials and methods

2.1. Materials

The human neuroblastoma SH-SY5Y cell line was provided by Dr. E. Stubbs, Jr. (Department of Neurology, Loyola University Medical Center). The Bradford dye for the protein assay was purchased from Bio-Rad Laboratories (Hercules, CA). Pure phospholipids were purchased from Avanti Polar Lipids (Alabaster, AL), and Nunclon TripleFlask flasks were from Fisher Scientific (Pittsburgh, PA). All other biochemicals and inorganic salts were purchased from Sigma Chemical Company (St. Louis, MO).

2.2. Preparation of human neuroblastoma SH-SY5Y cell fractions

Human neuroblastoma SH-SY5Y cells were grown for 4–6 weeks with 0, 2.5, or 5.0 mM LiCl supplemented in the growth medium and harvested as previously described [14]. We confirmed that the cells were viable in the absence and presence of up to 5.0 mM Li^+ (>90%) using a Trypan Blue test. The viability of neuroblastoma SH-SY5Y cells is unaltered after chronic Li^+ incubation [15]. For each fractionation method, the mixture of protease inhibitors consisted of 1.0 mM phenylmethylsulfonyl fluoride, 0.1 μM pepstatin, and 50.0 μM leupeptin [16]. All buffers were kept on ice during preparation, washing, and storage. Each final pellet was washed twice with 5.0 mM Tris–HCl (pH 7.3) buffer for plasma and nuclear membranes and microsomes or with 20 mM Tris–Cl (pH 7.4) and 145 mM tetramethylammonium chloride buffer for the intact organelles (nuclei and mitochondria). Membranes and intact organelles were stored at −80 °C for less than 2 weeks before use.

The cell homogenate was prepared by lysing of harvested cells in a 5.0 mM Tris–Cl buffer (pH 7.3). The cytosol and cytosol-free fractions were further purified from the cell homogenate fraction by centrifugation ($100,000 \times g$/60 min/4 °C), in which the resulting supernatant and pellet were used for the preparation of cytosol and cytosol-free fractions, respectively. In each case, the isolated fraction was washed

twice (100,000×g/60 min/4 °C), and the supernatants and the pellet were kept. The pellet was the cytosol-free cell fraction, whereas the supernatants were combined and concentrated by passage through a 3000 MW filter with a low-speed centrifuge to yield the cytosol fraction.

Two modified methods were used for isolating the plasma membrane fraction [17,18], in which the first pellet (obtained at low speed) was washed twice more and the supernatants were combined for the higher speed pelleting step to increase the total protein yield of the plasma membrane fraction. The nuclei were prepared as described previously [19]. For the nuclear membrane, first the nuclei were prepared [19] and then the nuclear membrane was isolated by a published procedure [20]. For the microsomal [21] and mitochondrial [22] isolations, the fractions were isolated as previously described.

2.3. Assays of subcellular fractions

To determine the protein concentration for each subcellular fraction, a modified Bradford protein assay with detergent was used [23]. The cytosol marker lactic dehydrogenase [24], the plasma membrane marker phosphodiesterase I [25], the mitochondrial marker succinate dehydrogenase [22], the nuclear marker DNA [26], and the microsomal marker NADH-cytochrome c reductase [22] were assayed as described previously.

The purification level – a measure of sample purity – of each subcellular fraction was obtained by dividing the specific activity of the particular sample by the specific activity of the cell homogenate. Thus, the specific activities of the enzymes and the amount of DNA in the different fractions were normalized to the specific activities of the same enzymes or to the amount of DNA in the cell homogenate fraction. We evaluated relative levels of purity or contamination by dividing the purification level of a particular enzyme or DNA by the sum of all the purification levels for a given subcellular fraction. For example, for the cytosol fraction, its relative purity was assessed by dividing the purification level of the cytosolic enzyme by the sum of all purification levels for the markers in the cytosol fraction.

2.4. Extraction of phospholipids and concentration determination

Phospholipids were extracted from membrane fractions [27] and dissolved in 400 μl chloroform/150 μl methanol/50 μl aqueous 0.2 M cesium-EDTA [28]. To assign phospholipids using ^{31}P NMR, we used a combination of values from the ^{31}P chemical shift literature in similar solvents [29,30] and of ^{31}P NMR samples spiked with pure phospholipids. For sample spiking, we added pure phospholipids, namely, PC, PC$_{AA}$, phosphatidylethanolamine plasmogen (PE$_P$), PE, PI, PS, and SM, to the phospholipid sample after the initial NMR experiment.

2.5. Instrumentation

^{7}Li NMR experiments were conducted with a Varian INOVA-300 NMR, a Varian VXR-300 NMR or a Varian VXR-400S NMR spectrometer equipped with multinuclear 10 mm broadband probes at 116.5 MHz or 155.3 MHz, respectively. Samples were run at 37 °C in 10-mm NMR tubes spinning at 18 Hz. ^{7}Li NMR T_1 relaxation measurements were conducted by use of the inversion recovery pulse sequence, $[D_1 - (180° - \tau - 90°)]_n$, whereas T_2 relaxation measurements were conducted by use of the Carr–Purcell–Meiboom–Gill sequence, $[D_1 - (90° - \tau - 180° - \tau)]_n$. Each relaxation value was determined with 7 interpulse delay values (τ), a number of transients ($n \geq 2$), an acquisition time of 0.979 s, a pre-acquisition delay (D_1) of 5 times the maximum expected T_1 value, and 19584 data points.

^{31}P NMR experiments on extracted phospholipids were conducted with a Varian VXR-400S NMR spectrometer equipped with a multinuclear 5 mm broad band-probe at 161.9 MHz with an acquisition time of 0.8 s, 2432 data points, a sweep width of 1518 Hz, a delay time of 1.2 s, a 45° pulse angle, and inverse-gated proton decoupling. Using the Varian INOVA-300 NMR spectrometer, we conducted ^{31}P NMR control experiments with a 90° pulse angle and a delay time of 10 s as well as experiments with a 45° pulse angle and a delay time of 1.2 s, the latter being the parameters used with the Varian VXR-400S NMR spectrometer. In both cases, the areas of the ^{31}P NMR phospholipid resonances were not significantly different, indicating that the shorter pulse and delay time used in all reported experiments were sufficient to ensure complete relaxation of all observed phospholipid peaks.

All UV/visible absorbance measurements necessary for assays of subcellular fractions and protein determinations were made on a Jasco Model V-500 spectrophotometer. We measured the sample viscosities with a Brookfied Cone Plate viscometer equipped with a 0.8° CP-40 cone at 12 rpm. For the cellular fractions, a 200 μM standard of polyvinyl-pyrrolidone (PVP, MW-360,000) was used for adjusting the viscosity of the sample to 5 cP; the value of 5 cP was chosen because this is a reasonable estimate of intracellular viscosity [31]. A Beckman J2-21 centrifuge with fixed-angle rotors (JA-14 or JA-20A) was used for the lower-speed cell fractionation procedures and for harvesting of cells. A Dupont RC 60 ultracentrifuge with a T-865 rotor was used for higher-speed procedures.

2.6. Determination of Li^+ binding from ^7Li NMR T_1 and T_2 relaxation rates

The ^{7}Li NMR T_1/T_2 ratio was used for determining qualitatively the degree of Li$^+$ immobilization in the different subcellular fractions [5,6,32]. In order to make the interpretation of our ^{7}Li NMR relaxation data under-

standable to those readers who are non-specialists in NMR spectroscopy, we briefly describe in this section the theoretical background necessary for evaluating our NMR relaxation results. The T_1 and T_2 NMR relaxation times of the ^{7}Li nucleus are dependent on the Li$^+$ rotational correlation time (τ_c), a scale of Li$^+$ motion, which is assumed to be isotropic. When the Li$^+$ ion is free, the τ_c value of ^{7}Li is short with respect to its NMR resonance frequency ω ($\omega\tau_c \ll 1$), resulting in $T_1 \approx T_2$. When Li$^+$ binds and as its immobilization increases, τ_c becomes larger, and when $\omega\tau_c \gg 1$ one observes that $T_1 > T_2$.

Only one type of Li$^+$ binding site is generally assumed to be present, as well as mono-exponential relaxation of the ^{7}Li nucleus and fast exchange of Li$^+$ between free and bound states [5,6,32]. These are reasonable assumptions, considering the high lability and low association constants of Li$^+$ binding, the lack of sensitivity of the chemical shift and relaxation times of the ^{7}Li nucleus to the type of coordinating atoms present in its binding site(s) and its small quadrupolar coupling constant, which lead to long relaxation times [5,6,32]. Relaxation of the ^{7}Li nucleus is governed by a major dipolar contribution, with a small quadrupolar contribution, due to its small quadrupolar coupling constant and the small distortions from axial symmetry expected for the Li$^+$ coordination with biological ligands [32]. Under these conditions, the major dipolar contribution to the ^{7}Li nucleus for the observed T_1 relaxation time is directly proportional to τ_c, whereas the observed T_2 relaxation is inversely proportional to τ_c [32]. Therefore, the ^{7}Li NMR T_1/T_2 relaxation ratio is directly proportional to τ_c^2, $(T_1/T_2)_{dd} \propto \tau_c^2$, making this ratio a valuable measure of the degree of Li$^+$ immobilization, which is independent of the fraction of bound Li$^+$ and Li$^+$ binding affinity [32].

Although the small quadrupolar contribution to ^{7}Li ($I=3/2$) relaxation could in principle be biexponential [33, 34], Li$^+$ bound to cells in fast exchange conditions is found to undergo mono-exponential relaxation [5]. Then, when $\omega\tau_c \gg 1$, again $(1/T_1)_q \propto q_{zz}\,\tau_c^{-1}$, $(1/T_2)_q \propto q_{zz}\,\tau_c$, so that $(T_1/T_2)_q \propto \tau_c^2$ (q_{zz} is the electrical field gradient at the nucleus, which is assumed to be axial) [35]. In contrast, the observation that the linewidth of the quadrupolar central transition ($-1/2 \Leftrightarrow +1/2$) of quadrupolar nuclei (e.g. ^{27}Al) in high-affinity metal ions bound to large proteins, such as transferrins, is proportional to τ_c^{-1}, or $T_2 \propto \tau_c$, in the slow tumbling limit [36,37], does not apply to the present ^{7}Li studies. Thus, the expression $(T_1/T_2) \propto \tau_c^2$ for ^{7}Li NMR constitutes a qualitatively reasonable approximation [32].

We first used the observed T_1 and T_2 values of subcellular fractions containing Li$^+$ at concentrations of 2.0, 4.0, 6.0, and 500 mM (see Table 2) to identify the major Li$^+$ binding sites in SH-SY5Y cells. For those fractions where major Li$^+$ binding was found, the observed T_1 values at Li$^+$ concentrations of 2.0, 4.0, 6.0, 8.0, 10, 12, and 500 mM were used to calculate the apparent Li$^+$ binding

constants (K_{Li}) to various human neuroblastoma fractions, with the assumption that Li$^+$ is either free or bound, and is undergoing a fast exchange between the two states [5,6,32].

$$R_{obs} = 1/T_{1(obs)}\ R_{free} = 1/T_{1(free)}\ R_{bound} = 1/T_{1(bound)} \quad (1)$$

$$\Delta R^{-1} = (R_{obs} - R_{free})^{-1} = K_{Li}^{-1}\{[B](R_{bound} - R_{free})\}^{-1}$$
$$+ [Li^+]\{[B](R_{bound} - R_{free})\}^{-1}, \quad (2)$$

where [Li$^+$] and [B] are the concentrations of Li$^+$ and membrane binding sites, respectively. R_{obs}, R_{free}, and R_{bound} are the relaxation rates (or the reciprocals of the relaxation times) for the Li$^+$ nuclei of the observed sample ($T_{1(obs)}$), with saturating Li$^+$ concentrations ($T_{1(free)}$) or with Li$^+$ bound ($T_{1(bound)}$), respectively. By using James–Noggle plots [38] in which ΔR^{-1} values are plotted against [Li$^+$], we determined K_{Li} by dividing the slope by the y-intercept. This approach has the inherent approximation of using a binding model with a single type of Li$^+$ binding site, with a single K_{Li} and R_{bound} value. Although the use of a distribution of binding sites might be more appropriate, that type of analysis is not feasible by this method. Thus, the single apparent Li$^+$ site is approximately equivalent to an average of the distribution of sites.

2.7. Human neuroblastoma membrane phospholipid quantification by ^{31}P NMR

The percentage of each phospholipid was determined by integration of the assigned resonances with normalization to 100% by use of the NMR software [12]. Once the phospholipid extract was measured by ^{31}P NMR, a known amount of pure phospholipid was added, and the extract was remeasured by ^{31}P NMR spectroscopy. All samples were spiked with a known concentration of PC, our internal reference, for determining the total phospholipid concentration, which was calculated from the following equation:

$$TP = \frac{A_P}{A_s} \times \frac{W_{PC}}{V_S} \times \frac{V}{V_m \times [Pro] \times PC\%}, \quad (3)$$

where TP corresponded to the total phospholipid per total protein concentration (mg phospholipid/ mg protein), W_{PC} was the known amount of added phospholipid (mg), and A_P and V were the area of the specific phospholipid peak from the ^{31}P NMR spectrum and the volume of the solvents that were used to dissolve the phospholipid extract, respectively. A_s and V_s were the peak area of the spiked phospholipid resonance and the volume of the sample after the addition of the pure phospholipid, and V_m corresponded to the initial volume of the phospholipid extract. [Pro] was the protein concentration of the extract, and PC% (v/v) was the percentage of phosphatidyl choline added to the phospholipid extract.

2.8. Data analysis

Data are expressed as means ± S.D. and $P < 0.05$ was considered significant. Statistical significance was determined by using a Student's t-test.

3. Results and discussion

3.1. Characterization of human neuroblastoma SH-SY5Y subcellular fractions

Before investigating the degree of Li^+ binding in the various subcellular fractions, we assayed enzymes or DNA specific to each individual organelle (see Materials and methods) for determination of the purity of each isolated subcellular fraction (Fig. 1). The enzyme or DNA assay data for the subcellular fractions were expressed as purification levels, with the cell homogenate fraction being assigned a value of 1 (Fig. 1); therefore, any fraction containing a purification factor greater than 1 (or less than 1) had more (or less) specific enzyme activity or DNA amount of that particular subcellular marker.

The cytosol fraction showed a significant increase ($P < 0.0005$) in the purification level of the cytosol marker enzyme (clear bar, Fig. 1) and a simultaneous significant decrease ($P < 0.0001$) in the activities of all the other enzyme or DNA markers (all statistical analyses in this paragraph are relative to the respective enzymatic marker assays of the cell homogenate fraction). The cytosol-free cell homogenate showed a significant decrease ($P < 0.0001$) in the purification level of the cytosol enzyme marker (clear bar), while showing significant increases in the purification levels of the markers
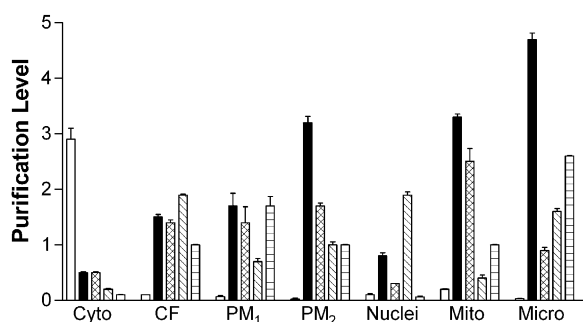

Fig. 1. Purification levels in human neuroblastoma SH-SY5Y cellular fractions. Purification levels are expressed in terms of enzyme or DNA markers present in each cell fraction. A purification level greater (or less) than 1 indicates more (or less) specific enzyme activity or amount of DNA of the marker in the particular subcellular fraction. The clear bar corresponds to the cytosol marker enzyme; the black bar to the plasma membrane marker enzyme; the hatched bar to mitochondrial purification level; the slanted striped bar to the nuclear marker; and the horizontally striped bar to the microsomal marker enzyme. The meanings of the fraction abbreviations are: Cyto, cytosol; CF, cytosol-free cell homogenate; PM_1, plasma membrane obtained from the procedure in ref. 15; PM_2, plasma membrane obtained from the procedure in ref. 16; Mito, mitochondria; and Micro, microsomes. Values represent means ± S.D. ($n = 3$).

for the PM ($P < 0.0004$), mitochondria ($P < 0.0014$), and nuclei ($P < 0.0001$). The purification level of microsomes in the cytosol-free fraction was not statistically different from that in the cell homogenate fraction ($P < 1.00$). One of the plasma membrane-enriched fractions, PM_1 [17], showed a significant increase ($P < 0.04$) in the purification level of the plasma membrane marker (black bar), with significant contamination ($P < 0.016$) of microsomes (horizontally striped bar). The other plasma membrane fraction, PM_2 [18], showed a greater significant increase ($P < 0.0001$) in the plasma membrane marker (black bar), with significant contamination ($P < 0.0004$) of mitochondria (gray bar). The nuclear fraction showed a significant increase ($P < 0.0001$) in the content of DNA (slanted striped bar), with significant contamination ($P < 0.03$) of the plasma membrane (black bar). For the mitochondrial fraction, there was a significant increase ($P < 0.003$) in the mitochondrial purification level (gray bar), but a significant contamination ($P < 0.0001$) of plasma membrane remained (black bar). The microsomal fraction showed a significant increase ($P < 0.0001$) in the microsomal marker (horizontally striped bar), with significant contamination ($P < 0.0001$ and $P < 0.0007$, respectively) of the plasma membrane (black bar) and nuclei (slanted striped bar).

3.2. Optimization of experimental conditions for Li^+ binding

Before examining Li^+ binding to the subcellular fractions, we performed control experiments on the cell homogenate to determine whether different factors (such as storage time of the sample, viscosity of the sample, and radiofrequency) significantly affected the ^7Li NMR T_1/T_2 ratios. We determined the ^7Li NMR T_1/T_2 ratio values (mean ± S.D., $n = 3$) for cell homogenate samples treated with Li^+ at concentrations of 2.0, 4.0, or 6.0 mM under 4 different experimental conditions (Table 1): (1) freshly prepared and used immediately; (2) stored for less than 2 weeks at −80.0 °C; (3) same as 2 with the viscosity adjusted to 5 cP (see Materials and methods); (4) same as 3, except a VXR-400S NMR spectrometer rather than a Varian VXR-300 NMR spectrometer was used. The ^7Li NMR T_1/T_2 ratios demonstrated no significant difference ($P > 0.05$) in the ratios at comparable Li^+ concentrations under the different conditions of storage, sample viscosity, and NMR radiofrequency. These observations indicate that no significant change in Li^+ immobilization occurs in the cell homogenate under these various conditions. For all remaining ^7Li NMR data described in this study, the selected experimental conditions for all of the subcellular samples were: storage for less than 2 weeks at −80.0 °C with the viscosity adjusted to 5 cP, with measurements performed on either a Varian VXR-300 or VXR-400 NMR spectrometer.

3.3. Li^+ binding to human neuroblastoma SH-SY5Y subcellular fractions

In Table 2, the ^7Li NMR T_1, T_2, and T_1/T_2 ratios are presented for the neuroblastoma subcellular fractions. The

Table 1
Optimization of the experimental conditions for the ^{7}Li NMR T_1, T_2, and T_1/T_2 relaxation measurements with human neuroblastoma cell homogenate fractions[a]

Conditions	[Li$^+$] (mM)	T_1 (s)	T_2 (s)	T_1/T_2
Freshly	2.0	14.7±0.6	0.18±0.02	84±5
prepared	4.0	16.0±0.7	0.25±0.02	65±8
	6.0	17.7±0.7	0.28±0.03	58±9
Stored for	2.0	15.1±0.8	0.19±0.01	78±3
less than	4.0	15.7±0.3	0.24±0.01	65±1
2 weeks	6.0	16.9±0.2	0.31±0.03	55±4
Stored for	2.0	14.2±0.2	0.16±0.02	87±10
less than	4.0	15.6±0.1	0.22±0.02	72±6
2 weeks with	6.0	16.0±0.3	0.28±0.01	57±1
viscosity adjusted				
(5 cP)				
Stored for	2.0	14.0±0.6	0.22±0.06	69±23
less than	4.0	15.6±1.4	0.28±0.04	58±9
2 weeks with	6.0	17.0±1.4	0.29±0.04	59±7
viscosity adjusted				
(to 5 cP) on				
VXR-400 NMR				

[a] Each value reported ($n=3$) represents the mean±S.D. For each [Li$^+$], the ^{7}Li NMR T_1, T_2, and T_1/T_2 ratio values are not significantly different ($P>0.05$). For all samples, the protein concentration was 8.0±0.5 mg/ml.

cytosol, nuclear and mitochondrial fractions were found to have small ^{7}Li NMR T_1/T_2 ratios. By contrast, large ^{7}Li NMR T_1/T_2 ratios were observed with the plasma membrane, microsomal, and cytosol-free cell homogenate

Table 2
T^{7}Li NMR T_1, T_2, and T_1/T_2 relaxation values for subcellular fractions of human neuroblastoma cells[a]

Fraction	[Li$^+$] (mM)	T_1 (s)	T_2 (s)	T_1/T_2
Cytosol-free cell	2.0	7.5±0.2	0.09±0.02	82±16
homogenate	4.0	8.6±0.5	0.12±0.01	74±3
	6.0	8.9±0.4	0.13±0.01	70±6
Cytosol-enriched	2.0	11.2±1.2	1.6±0.04	7±0.1
fraction	4.0	12.1±0.6	2.0±0.04	6±0.3
	6.0	12.8±0.7	2.4±0.33	5±1.0
Plasma membrane-enriched	2.0	8.9±0.5	0.07±0.01	129±13
fraction [17][b,*]	4.0	9.7±0.6	0.09±0.01	106±12
	6.0	10.8±1.0	0.11±0.01	96±10
Plasma membrane-enriched	2.0	11.2±0.5	0.04±0.01	323±41
fraction [18][b,*]	4.0	12.7±0.9	0.05±0.01	264±30
	6.0	13.8±0.9	0.07±0.01	185±12
Nuclear-enriched	2.0	9.5±0.4	0.60±0.04	16±2
fraction	4.0	11.6±0.5	0.80±0.12	15±3
	6.0	12.6±1.4	1.4±0.2	9±1
Mitochondria-enriched	2.0	14.6±0.8	1.0±0.1	15±2
fraction	4.0	16.6±1.6	1.2±0.1	14±3
	6.0	15.9±0.2	1.3±0.1	12±1
Microsome-enriched	2.0	13.6±0.8	0.16±0.04	87±24
fraction*	4.0	15.0±1.2	0.32±0.15	52±17
	6.0	15.6±0.4	0.39±0.12	42±10

[a] Each value ($n=3$) reported represents the mean±S.D. Samples were stored at −80.0 °C for less than 2 weeks before use. Viscosity was adjusted to 5.0±0.5 cP with PVP-360, and the protein concentration was 8.0±0.5 mg/ml.
[b] The difference between the two different plasma membrane fractions is in the procedures by which they were isolated (see Materials and methods).
* $P<0.001$, significant differences in I_1/I_2 ratio values.

fractions. Further examination of Li$^+$ binding was done by determination of Li$^+$ binding affinities via James–Noggle plots (see Fig. 2A and Materials and methods). The Li$^+$ binding constants for the two Li$^+$-treated plasma membrane fractions, PM$_1$ and PM$_2$, were 272.2±61.4 M^{-1} ($r^2=0.92$; $n=3$) and 341.2±48.4 M^{-1} ($r^2=0.95$; $n=4$), respectively (mean±S.D.). The Li$^+$ binding constant to the microsome-enriched fraction was 165.5±54.3 M^{-1} (mean±S.D., $r^2=0.94$; $n=4$).

Thus, Li$^+$-treated cytosol-enriched fractions, which contained a small contamination from other fractions (~31% total contamination), had significantly smaller ^{7}Li NMR T_1/T_2 values than the cytosol-free fractions titrated with the same Li$^+$ concentrations, indicating more Li$^+$ binding in the absence of cytosol. Even though the cytosol-enriched fraction showed little Li$^+$ binding, the amount of Li$^+$ binding sites may be slightly underestimated, because during the isolation of these fractions, many small biomolecules, such as ATP, which are known to exhibit some Li$^+$ binding [39], may become hydrolyzed. Therefore, we conclude that the cytosol-free fraction contains the major Li$^+$ binding sites in SH-SY5Y cells.
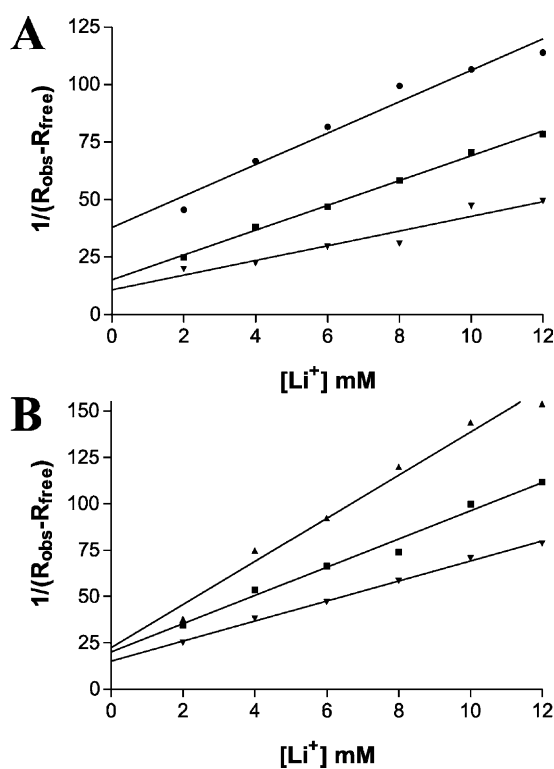

Fig. 2. Representative James–Noggle plots of (A) the plasma membrane fraction PM$_1$ (▼), the plasma membrane fraction PM$_2$ (■) and the microsome fraction (●), and B) the plasma membrane PM$_2$ fractions under Li$^+$-free (▼) and chronic conditions at 2.5 mM (■) and 5.0 mM LiCl (▲). The x-axis corresponds to LiCl concentrations used in the titrations of the membrane samples and the y-axis represents $1/(R_{obs}-R_{free})$, where R_{obs} and R_{free} are the relaxation rates (or the reciprocals of the relaxation times) for the Li$^+$ nuclei of the observed sample ($T_{1(obs)}$) and with saturating Li$^+$ concentrations ($T_{1(free)}$), respectively. By plotting ΔR^{-1} vs. [Li$^+$], K_{Li} values are derived by dividing the slope by the y-intercept.

By using additional fractionation procedures, we isolated subcellular fractions within the cytosol-free cell homogenate fraction and examined them for Li^+ binding. As illustrated in Table 2, the greatest ^7Li NMR T_1/T_2 ratios occurred with both plasma membrane and microsomal fractions. Two different isolation procedures were used for obtaining the plasma membrane fraction. For the first plasma membrane fraction (PM_1), mitochondrial and microsomal contaminations were detected ($\sim25\%$ and $\sim31\%$, respectively). In the PM_2 fraction, however, the contamination from the microsomes was $\sim14.5\%$, and the amount of mitochondria remained the same ($\sim25\%$) as for the PM_1 fraction. Overall, the PM_2 fraction had a higher purity ($\sim46\%$) as compared to the PM_1 ($\sim31\%$). Therefore, as the plasma membrane enrichment increases, more Li^+ binding occurs, as indicated by the significantly larger ^7Li NMR T_1/T_2 ratios obtained with PM_2 fractions relative to those of PM_1 fractions titrated with the same Li^+ concentrations ($P<0.001$; Table 2). The other fraction that contained significant Li^+ binding was the microsomal fraction, which was contaminated with plasma membrane and nuclei ($\sim48\%$ and $\sim16\%$, respectively). Surprisingly, the microsome-enriched fraction had the largest amount of the enzymatic marker for the plasma membrane as compared to the other fractions, and yet, it had a significantly smaller ^7Li NMR T_1/T_2 ratio than did the PM_2 fraction ($P<0.001$). From these data alone, it is unclear whether the larger ^7Li NMR T_1/T_2 ratio of the PM_2 fraction as compared to the microsomal fraction is due to the presence of the plasma membrane or of microsomes alone, or to both. Because of the significant plasma membrane contamination in the microsomal fraction, the attribution of Li^+ binding to microsomes needs to be interpreted with caution.

To test the hypothesis that Li^+ binding is specific to membrane fractions in general, we isolated the nuclear membrane from the nuclear-enriched fraction. The nuclear membrane fraction was assumed to have a high purity, because it was obtained from the intact nuclear fraction, which had a purity of $\sim60\%$. This fraction was titrated with LiCl at the concentrations of 2.0, 4.0, or 6.0 mM, yielding ^7Li NMR T_1/T_2 ratios (mean±S.D., $n=3$) of 38 ± 6, 26 ± 1, or 27 ± 6, respectively. As compared to the nuclear fraction (see Table 2), the ratio values of the nuclear membrane samples were significantly larger for each Li^+ concentration investigated ($P<0.007$). Therefore, the nuclear membrane binds Li^+ to a greater degree than does the intact nuclear fraction. Based on the ^7Li NMR binding data obtained with nuclear fractions and nuclear membrane samples, we conclude that membrane domains are the major Li^+ binding sites in neuronal systems. In support of this conclusion, the mitochondria-, cytosol-, and nuclear-enriched fractions exhibited much smaller ^7Li NMR T_1/T_2 ratios and hence lower levels of Li^+ binding and immobilization. Even though the mitochondria-enriched fraction contained a significant contamination of plasma membrane ($\sim45\%$), the ^7Li NMR T_1/T_2 ratio was small, presumably due to the presence of intact mitochondria. Moreover, the intact nuclear fraction, which was relatively pure ($\sim60\%$), had small ^7Li NMR T_1/T_2 ratios. Even though these intact organelles are not major Li^+ binding sites, there may be major Li^+ binding sites within these organelles, as indicated by the increase in the T_1/T_2 ratios of the nuclear membrane fractions as compared to those in intact nuclei.

The above analysis of T_1/T_2 ratios is generally confirmed by the relative values of the T_2 data (Table 2), as the relative order of T_1/T_2 ratios is virtually the same (inverted) as that of T_2. This is because the effect of τ_c on T_1 is much smaller than on T_2, so the latter dominates the ratio.

3.4. Percentage of phospholipids in the subcellular fractions

We determined the phospholipid composition in the plasma membrane and cell homogenate fractions of human neuroblastoma SH-SY5Y cells and the effect of chronic Li^+ treatment on their phospholipid concentrations because: (1) the major Li^+ binding sites were present in membrane domains, (2) the phospholipids are major Li^+ binding sites within membranes [12], (3) the plasma membrane composition of this cancer cell line has been shown not to be significantly altered compared to normal neuronal tissue [40], and (4) Li^+ treatment has been hypothesized to alter phospholipid levels [7,9]. We chose to investigate the plasma membrane fraction because it had the highest Li^+ binding affinity, as compared to the microsomal and nuclear membrane fractions. Additionally, we used the second method of plasma membrane purification [18] because it gave the largest yield of plasma membrane, and with the highest purity (Fig. 1). Fig. 3 shows a representative ^{31}P NMR spectrum of phospholipids purified from the plasma membrane-enriched fraction obtained from Li^+-free cells.

We compared the phospholipid composition in the plasma membrane fraction to the cell homogenate to examine

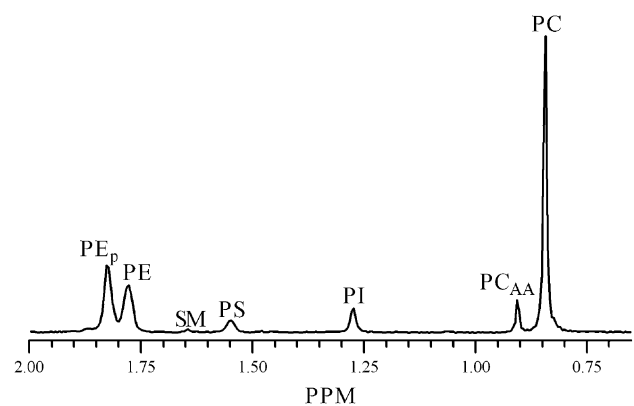Fig. 3. ^{31}P NMR spectrum of a phospholipid extract from the plasma membrane-enriched fraction in Li^+-free cells. The following phospholipids are identified: phosphatidylethanolamine plasmogen (PE_P), phosphatidylethanolamine (PE), spingomyelin (SM), phosphatidylserine (PS), phosphatidylinositol (PI), β-acyl-γ-alkylphosphatidylcholine (PC_{AA}), and phosphatidylcholine (PC). PC was the internal reference for each spectrum and was set to 0.84 ppm.

Table 3
Phospholipid composition (%) of the human neuroblastoma cell homogenate and plasma membrane fraction in the absence (0 mM LiCl) or after chronic treatment of cells with 2.5 and 5.0 mM Li$^+$ for 4 to 6 weeks[a]

	Cell homogenate fractions ($n=6$)			Plasma membrane-enriched fractions ($n=4$)		
[Li$^+$] mM	0	2.5	5.0	0	2.5	5.0
PS	4.8±1.2	4.5±0.6	3.2±0.8[b]	4.0±1.4	1.5±0.6[c]	1.5±0.6[c]
PI	8.0±0.6	8.2±0.8	9.7±0.5[d]	6.8±1.5	9.8±0.5[e]	10.3±1.0[f]
PC	48.0±1.1	47.2±2.6	47.0±3.0	44.0±8.9	42.0±3.4	41.5±4.2
PC$_{AA}$	12.2±0.8	10.2±1.0	9.2±2.8	8.3±4.0	9.5±2.4	7.8±1.7
SM	3.0±0.9	2.2±0.8	3.0±0.6	1.0±0.8[g]	1.3±0.5	1.0±0
PE[h]	24.3±1.9	28.2±3.1[i]	28.2±1.5[j]	35.3±5.1[g]	36.8±3.2	38.0±5.4
[PLP][k]	5.3±0.8	6.5±3.0	6.6±2.2	16.0±3.4[l]	11.6±3.4	11.7±2.6

[a] Each reported value is expressed as mean±S.D. The total areas under the ^{31}P NMR phospholipids resonances were normalized to 100%.

[b] $P<0.02$, significant differences in PS and PI levels for cell homogenate fractions that were Li$^+$-free and those that were preincubated with 5.0 mM LiCl.

[c] $P<0.03$, significant difference in PS levels for plasma membrane fractions that were Li$^+$-free and those that were preincubated with either 2.5 mM or 5.0 mM LiCl.

[d] $P<0.001$, significant differences in PS and PI levels for cell homogenate fractions that were Li$^+$-free and those that were preincubated with 5.0 mM LiCl.

[e] $P<0.02$, significant differences in PS levels for plasma membrane fractions that were Li$^+$-free and those that were preincubated with either 2.5 mM or 5.0 mM LiCl.

[f] $P<0.01$, significant differences in PS levels for plasma membrane fractions that were Li$^+$-free and those that were preincubated with either 2.5 mM or 5.0 mM LiCl.

[g] $P<0.05$, significant differences between Li$^+$-untreated plasma membrane and cell homogenate fractions in SM or PE, and PLP levels.

[h] PE represents the sum of the partially resolved PE and PE$_P$ resonances.

[i] $P<0.03$, significant difference in PE levels for cell homogenate fractions that were Li$^+$-free and those that were preincubated with 2.5 mM and 5.0 mM LiCl.

[j] $P<0.003$, significant difference in PE levels for cell homogenate fractions that were Li$^+$-free and those that were preincubated with 2.5 mM and 5.0 mM LiCl.

[k] [PLP] indicates the total phospholipid concentration (in mg of phospholipid per mg of protein).

[l] $P<0.04$, significant differences between Li$^+$-untreated plasma membrane and cell homogenate fractions in SM or PE, and PLP levels.

whether differences existed. The normalized percentages for the phospholipids PS, PI, PC, PC$_{AA}$, SM, and PE are shown in Table 3. Comparison under Li$^+$-free conditions of the phospholipid levels between the cell homogenate and the plasma membrane showed that PE levels were significantly larger ($P<0.05$), whereas SM levels were significantly smaller ($P<0.05$) in the plasma membrane relative to those in the cell homogenate; no significant differences ($P>0.05$) were found for the other phospholipids. The total phospholipid concentration in the plasma membrane fractions was significantly larger than that in the cell homogenate ($P<0.04$), as expected, because phospholipids reside primarily in the plasma membrane and are concentrated after centrifugation and enrichment from cell homogenate fractions.

We also determined how chronic Li$^+$ treatment affects the phospholipid levels in these two fractions. In the cell homogenate fraction, incubation with 5.0 mM LiCl significantly lowered the concentration of PS ($P<0.02$) and significantly increased the concentration of PI ($P<0.001$) as compared to Li$^+$-free samples. In the presence of either 2.5 or 5.0 mM Li$^+$ in the cell homogenate fractions, PE was significantly increased ($P<0.03$ or $P<0.003$, respectively) as compared to that in samples that were not subject to Li$^+$ preincubation. In the plasma membrane fraction, 2.5 or 5.0 mM Li$^+$ incubation was accompanied by a statistically significant decrease in the concentration of PS ($P<0.03$ in both cases) and a significant increase in the concentration of PI ($P<0.02$ and $P<0.01$, respectively) as compared to those in Li$^+$-free controls. Li$^+$ incubation did not produce any

significant change in total phospholipid concentration after chronic incubation with either 2.5 or 5.0 mM LiCl in both the cell homogenate ($P<0.4$ and $P<0.2$, respectively) and the plasma membrane fractions ($P<0.1$ and $P<0.09$, respectively) as compared to fractions that were not preincubated with Li$^+$.

Determination of phospholipid composition in synaptic plasma membranes from rat brain by two-dimensional thin-layer chromatography showed decreases in PS levels upon Li$^+$ incubation, in agreement with our observations, but, in contrast to our findings, no significant changes in PI levels [41]. Other studies have reported a decrease in PI levels [42,43], whereas other investigations did not observe any significant changes in PI [44,45] or inositol [46], its precursor, upon exposure to Li$^+$. In agreement with our measures, however, a recent study that used ^{31}P magnetic resonance spectroscopic imaging of the human brain of healthy subjects, also reported an increase in phosphomonoesters, including PI, following lithium administration [47].

Contradictory findings on the effect of Li$^+$ on PI and inositol levels may have multiple reasons, including: (1) the accuracies and sensitivities of the different analytical tools used in separate laboratories. A large number of studies on the phospholipid composition of membranes and inositol metabolism have used two-dimensional thin-layer chromatography [41,42,44,45] or HPLC [46], which are methods that can only be used for quantitative analysis with great difficulty [43]. In contrast, the accuracy of the ^{31}P NMR method for the analysis of the phospholipid composition of membranes has long been established [27–30,43,47,48],

with measurements in vitro [27–30] being more accurate than those in vivo [43,47,48]. Nonetheless, the ^{31}P NMR method also has its shortcomings. Because of the inherently low sensitivity of NMR spectroscopy, discrepancies have also been observed in studies using the ^{31}P NMR method. For example, whereas the most recent study by Yildiz et al. [47] found an increase in phosphomonoester concentration, previous studies using the same methodology observed either a decrease [43,49] or no change [50] in PI levels; the sensitivity problem was, however, addressed in the most recent study [47] that observed an increase in phosphomonoester levels by collecting data from a larger volume of the human brain and by using proton-decoupled ^{31}P NMR spectroscopy; other reasons include: (2) interspecies differences in PI metabolism [51]; (3) regional brain differences in inositol metabolism [46,52]; 4) differences in response of the PI pathway to the length of time of Li^{+} treatment [52]; and altered signaling pathways in bipolar patients [53].

According to the inositol depletion hypothesis for Li^{+} action [54], Li^{+} uncompetitively inhibits inositol mono-phosphatase, thereby increasing the levels of inositol phosphates and decreasing the concentrations of inositol, which would presumably lead to a slowing down of the resynthesis of inositol-containing metabolites (including PI) needed for signal transduction. This hypothesis has been challenged because inositol is ubiquitous in the brain and its concentration is above that of the K_m value for phospha-tidylinositol synthase, the enzyme responsible for the resynthesis of PI from inositol and cytidine diphosphodia-cylglycreol [1,55]. Recent re-evaluations of the inositol depletion hypothesis [1,47,55] allow for the possibility of lower inositol levels in overstimulated brain cells that trigger events at several levels of gene expression and signal transduction, including ongoing or enhanced PI resynthesis. An alternative explanation for our observed increase in PI levels upon Li^{+} incubation may involve the inhibition of guanine nucleotide-binding (G) proteins by Li^{+} [56]. At therapeutic levels, Li^{+} inhibits G_q, the signaling protein responsible for the activation of phospholipase C [56]. The decreased activation of phospholipase C may result in inhibition of the hydrolysis of phosphatidylinositol-4,5-bisphosphate and the concomitant accumulation of PI levels. Future studies will explore the mechanism(s) responsible for the increase in PI levels observed in SH-SY5Y cells upon Li^{+} incubation.

Chronic incubation with either 2.5 or 5.0 mM LiCl resulted in K_{Li} of the plasma membrane-enriched fractions of 363.9 ± 36.3 and 493.8 ± 63.8 M^{−1} (mean ± S.D., $r^2 = 0.92$ and 0.94, $n = 4$), respectively (Fig. 2B). The Li[+] binding constant to the plasma membrane incubated with 2.5 mM LiCl was not significantly different ($P < 0.48$), but the Li^{+} binding constant to the plasma membrane incubated with 5.0 mM LiCl was significantly different ($P < 0.009$) from that measured for plasma membrane samples without prior Li^{+} incubation (341.2 ± 48.4 M^{−1}, mean ± S.D., $r^2 = 0.95$, $n = 4$). At physiological pH, the headgroups of both PS and PI carry a

net negative charge and should therefore have considerable affinity for Li^{+}. From ^{31}P NMR titrations of pure PS and PI suspensions with Li^{+}, we found that the affinity of Li^{+} for PS is approximately 20% larger than that of PI [12]. The approximate 60% decrease in PS present in the plasma membrane extracted from SH-SY5Y cells that were preincubated with 5.0 mM LiCl is not fully compensated by the approximate 50% increase in PI. Based solely on the relative affinities of Li^{+} for pure PS and PI phospholipids in suspension and the relative phospholipid compositions of plasma membranes extracted from cells with and without preincubation with LiCl, one would predict that the plasma membrane isolated from SH-SY5Y cells that were preincubated with 5.0 mM LiCl would be smaller than that for membrane without any LiCl preincubation. The opposite trend was instead observed because the relative affinities of PS and PI for Li^{+} in suspensions of pure phospholipids are not accurate representations of the interactions of Li^{+} with headgroups of PS and PI embedded in a membrane bilayer. Indeed, ^{2}H NMR studies of liposomes containing a mixture of PS and PC showed that the Li^{+} distribution in the headgroup region of the anionic PS phospholipid is more buried than for the neutral PC phospholipid [57].

4. Concluding remarks

Similar to other physiologic ions such as Na^{+}, K^{+}, and Ca^{2+}, Li^{+} very likely has access to most intracellular domains, and the location(s) of Li^{+} is (are) probably driven by its electrostatic attraction to major intracellular structures bearing an excess negative charge. By identification of the intracellular location and binding sites of Li^{+}, the understanding of the biochemical action of Li^{+} at the intracellular level and its implications for the hypothesized mechanisms can be further evaluated.

In this report, we have provided evidence by ^{7}Li and ^{31}P NMR measurements that membrane domains are the major intracellular Li^{+} binding sites and that the phospholipid composition of the plasma membrane is altered upon Li^{+} incubation. The contributions of other potential anionic binding sites for Li^{+} binding, such as sialic acid residues bound to carbohydrates at the membrane surface and of negatively charged amino acid residues, were not explored in this study.

Progress in lithium research has been hampered by the unavailability of sensitive tools that can probe *directly* the Li^{+} interactions in cells and with macromolecules at therapeutically relevant Li^{+} concentrations. Although we used advanced spectroscopic techniques in this investigation, in this study, like in many others, it was not possible to probe Li^{+} interactions at the lower concentrations used in lithium therapy. Other more sensitive approaches, such as fluorescence microscopy and spectroscopy, will be necessary for the direct visualization of the location of Li^{+} within the cell. Currently, a Li^{+}-sensitive fluorescent probe is

unavailable; however, because Li^+ competes with other ions such as Mg^{2+}, examination of the intracellular location of Li^+ binding is sometimes possible through the use of indirect Mg^{2+}-sensitive probes [14,32].

Acknowledgements

References

[1] N.J. Birch, The medical use of lithium, in: A. Sigel, H. Sigel (Eds.), Metal Ions in Biological Systems, vol. 41, Marcel Dekker, Inc., New York, 2004, pp. 305–332.

[2] J.J.R. Frausto da Silva, R.J.P. Williams, Possible mechanism for the biological action of lithium, Nature 263 (1976) 237–239.

[3] J.W. Pettegrew, J.F.M. Post, K. Panchalingam, G. Withers, D.E. Woessner, ^7Li NMR study of normal human erythrocytes, J. Magn. Reson. 71 (1987) 504–519.

[4] J.W. Pettegrew, J.W. Short, R.D. Woessner, S. Strychor, D.W. McKeag, J. Armstrong, N.J. Minshew, A.J. Rush, The effect of lithium on the membrane molecular dynamics of normal human erythrocytes, Biol. Psychiatry 22 (1987) 857–871.

[5] Q. Rong, M.C.T. Espanol, D. Mota de Freitas, C.F.G.C. Geraldes, ^7Li NMR relaxation study of Li^+ binding in human erythrocytes, Biochemistry 32 (1993) 13490–13498.

[6] J. Nikolakopoulos, C. Zachariah, D. Mota de Freitas, E.B. Stubbs Jr., R. Ramasamy, M.M.C.A. Castro, C.F.G.C. Geraldes, ^7Li nuclear magnetic resonance study for the determination of Li^+ properties in neuroblastoma SH-SY5Y cells, J. Neurochem. 71 (1998) 1676–1683.

[7] H.L. Meltzer, Is there a specific membrane defect in bipolar disorders, Biol. Psychiatry 30 (1991) 1071–1074.

[8] G.N. Pandey, D.G. Ostrow, M. Haas, E. Dorus, R.C. Casper, J.M. Davis, D.C. Tosteson, Abnormal lithium and sodium transport in erythrocytes of a manic patient and some members of his family, Proc. Natl. Acad. Sci. U. S. A. 74 (1977) 3607–3611.

[9] D. Mota de Freitas, A. Abraha, Q. Rong, J. Silberberg, W. Whang, G.F. Borge, E. Elenz, Relationship between lithium ion transport and phospholipid composition in erythrocytes from bipolar patients receiving lithium carbonate, Lithium 5 (1994) 29–39.

[10] B.E. Ehrlich, J.M. Diamond, L. Gosenfeld, Lithium-induced changes in sodium-lithium countertransport, Biochem. Pharmacol. 30 (1981) 2539–2543.

[11] J.M. Diamond, K. Meier, L.F. Gosenfeld, R.S. Jope, D.J. Jenden, S.M. Wright, Recovery of erythrocyte Li^+/Na^+ countertransport and choline transport from lithium therapy, J. Psychiatr. Res. 17 (1982) 385–393.

[12] C. Srinivasan, N. Minadeo, C.F.G.C. Geraldes, D. Mota de Freitas, Competition between Li^+ and Mg^{2+} for red blood cell membrane phospholipids: a ^{31}P, ^7Li, and ^6Li nuclear magnetic resonance study, Lipids 34 (1999) 1211–1221.

[13] L.P. Montezinho, C.B. Duarte, C.P. Fonseca, Y. Glinka, B. Layden, D. Mota de Freitas, C.F.G.C. Geraldes, M.M.C.A. Castro, Intracellular

[14] A.M. Abukhdeir, B.T. Layden, N. Minadeo, F.B. Bryant, E.B. Stubbs, D. Mota de Freitas, Effect of chronic Li^+ treatment on free intracellular Mg^{2+} in human neuroblastoma SH-SY5Y cells, Bipolar. Disord. 5 (2003) 6–13.

[15] M.K. Patterson, Measurement of growth and viability of cells in culture, Methods Enzymol. 58 (1979) 141–152.

[16] W.A. Maltese, K.M. Sheridan, Isoprenylated proteins in cultured cells: subcellular distribution and changes related to altered morphology and growth arrest induced by mevalonate deprivation, J. Cell. Physiol. 133 (1987) 471–481.

[17] E. Knight, T.J. Connors, R. Hudkins, A.C. Maroney, N. Neff, Membranes of human neuroblastoma SH-SY5Y cells contain specific binding sites for [^3H]K-252A, Biochem. Biophys. Res. Commun. 211 (1995) 511–518.

[18] E.M. Costa, B.B. Hoffmann, G.H. Loew, Opioid agonists binding and responses in SH-SY5Y cells, Life Sci. 50 (1992) 73–81.

[19] R.I. Bolla, D.C. Braaten, Y. Shiomi, M.B. Hebert, D. Schlessinger, Localization of specific rDNA spacer sequences to the mouse L-cell nucleolar matrix, Mol. Cell. Biol. 5 (1985) 1287–1294.

[20] R.R. Kay, D. Fraser, I.R. Johnston, A method for the rapid isolation of nuclear membranes from rat liver. Characterisation of the membrane preparation and its associated DNA polymerase, Eur. J. Biochem. 30 (1972) 145–154.

[21] T. Jean, C.B. Klee, Calcium modulation of inositol 1,4,5-trisphosphate-induced calcium release from neuroblastoma x glioma hybrid (NG108-15) microsomes, J. Biol. Chem. 261 (1986) 16414–16420.

[22] W.A. Maltese, J.R. Aprille, Relation of mevalonate synthesis to mitochondrial ubiquinone content and respiratory function in cultured neuroblastoma cells, J. Biol. Chem. 260 (1985) 11524–11529.

[23] B.O. Fanger, Adaptation of the Bradford protein assay to membrane-bound proteins by solubilizing in glucopyranoside detergents, Anal. Biochem. 162 (1987) 11–17.

[24] A. Pesce, R.H. Mckay, F. Stolzenbach, R.D. Cahn, N.O. Kaplan, The comparative enzymology of lactic dehydrogenase, J. Biol. Chem. 239 (1963) 1753–1761.

[25] P.A. Butcher, L.W. Steele, M.R. Ward, R.E. Oliver, Transport of sodium into apical membrane vesicles prepared from fetal sheep alveolar type II cells, Biochim. Biophys. Acta 980 (1989) 50–55.

[26] K. Burton, A study of the conditions and mechanism of the diphenylamine reaction for the colorimetric estimation of deoxyribonucleic acid, J. Biochem. 62 (1956) 315–323.

[27] P. Meneses, T. Glonek, High resolution ^{31}P NMR of extracted phospholipids, J. Lipid Res. 29 (1988) 679–689.

[28] C. Srinivasan, N. Minadeo, J. Toon, D. Graham, D. Mota de Freitas, C.F.G.C. Geraldes, Competition between Na^+ and Li^+ for unsealed and cytoskeleton-depleted human red blood cell membrane: a ^{23}Na multiple quantum filtered and ^7Li NMR relaxation study, J. Magn. Reson. 140 (1999) 206–217.

[29] H.T. Edzes, T. Teerlink, M.S. van der Knaap, J. Valk, Analysis of phospholipids in brain tissue by ^{31}P NMR at different compositions of the solvent system chloroform–methanol–water, Magn. Reson. Med. 26 (1992) 46–59.

[30] T.E. Merchant, T. Glonek, ^{31}P NMR of phospholipid glycerol phosphodiester residues, J. Lipid Res. 31 (1990) 479–486.

[31] P.D. Morse, D.M. Lusczakoski, D.A. Simpson, Internal microviscosity of red blood cells and hemoglobin-free resealed ghosts: a spin-label study, Biochemistry 18 (1979) 5021–5029.

[32] B.T. Layden, A.M. Abukhdeir, N. Williams, C.P. Fonseca, L. Carroll, M.M.C.A. Castro, C.F.G.C. Geraldes, F.B. Bryant, D. Mota de Freitas, Effects of Li^+ transport and Li^+ immobilization on Li^+/Mg^{2+} competition in cells: implications for bipolar disorder, Biochem. Pharmacol. 66 (2003) 1915–1924.

[33] W.D. Rooney, C.S. Springer Jr., A comprehensive approach to the analysis and interpretation of the resonances of spins 3/2 from living systems, NMR Biomed. 4 (1991) 209–226.

[34] W.D. Rooney, C.S. Springer Jr., The molecular environment of intracellular sodium: ^{23}Na NMR relaxation, NMR Biomed. 4 (1991) 227–245.

[35] J.W. Akitt, The alkali and alkaline earth metals, in: J. Mason (Ed.), Multinuclear NMR, Plenum Press, New York, 1987, pp. 171–185.

[36] L.G. Werbelow, NMR dynamic frequency shifts and the quadrupolar interaction, J. Chem. Phys. 70 (1979) 5381–5383.

[37] J.M. Aramini, H.J. Vogel, The effects of temperature, viscosity and molecular size on the aluminium-27 QCT NMR of transferrins, J. Magn. Reson., B 110 (1996) 182–187.

[38] T.L. James, J.H. Noggle, [23]Na nuclear magnetic resonance relaxation studies of sodium ion interaction with soluble RNA, Proc. Natl. Acad. Sci. U. S. A. 62 (1969) 644–649.

[39] D. Mota de Freitas, L. Amari, C. Srinivasan, Q. Rong, R. Ramasamy, A. Abraha, C.F. Geraldes, M.K. Boyd, Competition between Li^+ and Mg^{2+} for the phosphate groups in the human erythrocyte membrane and ATP: an NMR and fluorescence study, Biochemistry 33 (1994) 4101–4110.

[40] E.B. Stubbs Jr., R.O. Carlson, C. Lee, S.K. Fisher, A.K. Hajra, B.W. Agranoff, Essential fatty acid deficiency in cultured SK-N-SH human neuroblastoma cells, Adv. Exp. Med. Biol. 318 (1992) 171–182.

[41] B. López-Corcuera, C. Giménez, C. Aragón, Change of synaptic membrane lipid composition and fluidity by chronic administration of lithium, Biochim. Biophys. Acta 939 (1988) 467–475.

[42] D. Ding, M.L. Greenberg, Lithium and valproate decrease the membrane phosphatidylinositol/phosphatidylcholine ratio, Mol. Microbiol. 47 (2003) 373–381.

[43] J.W. Pettegrew, K. Panchalingam, R.J. McClure, S. Gershon, L.R. Muenz, J. Levine, Effects of chronic lithium administration on rat brain phosphatidylinositol cycle constituents, membrane phospholipids and amino acids, Bipolar. Disord. 3 (2001) 189–201.

[44] J.C. Soares, A.G. Mallinger, C.S. Dippold, E. Frank, D.J. Kupfer, Platelet membrane phospholipids in euthymic bipolar disorder patients: are they affected by lithium treatment, Biol. Psychiatry 45 (1999) 453–457.

[45] M.P. Honchar, K.E. Ackermann, W.R. Sherman, Chronically administered lithium alters neither myo-inositol monophosphatase activity nor phosphoinositide levels in rat brain, J. Neurochem. 53 (1989) 590–594.

[46] B. Lubrich, Y. Patishi, O. Kofman, G. Agam, M. Berger, R.H. Belmaker, D. Van Calker, Lithium-induced inositol depletion in rat brain after chronic treatment is restricted to the hypothalamus, Mol. Psychiatry 2 (1997) 407–412.

[47] A. Yildiz, C.M. Demopoulos, C.M. Moore, P.F. Renshaw, G.S. Sachs, Effect of lithium on phosphoinositide metabolism in human brain: a proton decoupled ^{31}P magnetic resonance spectroscopy study, Biol. Psychiatry 50 (2001) 3–7.

[48] J.M. Pearce, R.A. Komorowski, Analysis of phospholipid molecular species in brain by ^{31}P NMR spectroscopy, Magn. Reson. Med. 44 (2000) 215–223.

[49] J.C. Soares, A.G. Mallinger, C.S. Dippold, K. Forster Wells, E. Frank, D.J. Kupfer, Effects of lithium on platelet membrane phosphoinositides in bipolar disorder patients. A pilot study, Psychopharmacology 149 (2000) 12–16.

[50] T. Kato, S. Takahashi, T. Shiori, T. Inubushi, Alterations in brain phosphorous metabolites in bipolar disorder detected by in vivo ^{31}P and [7]Li magnetic resonance spectroscopy, J. Affective Disord. 27 (1993) 53–60.

[51] M.A. Yorek, Biological distribution, in: G. Cevc (Ed.), Phospholipids Handbook, Marcel Dekker, Inc., New York, 1993, pp. 745–775.

[52] D. Van Calker, R.H. Belmaker, The high affinity inositol transport system—Implications for the pathophysiology and treatment of bipolar disorder, Bipolar. Disord. 2 (2000) 102–107.

[53] C.M. Moore, J.L. Breeze, S.A. Gruber, S.M. Babb, B.B. Frederick, R.A. Villafuerte, A.L. Stoll, J. Hennen, D.A. Yurgelun-Todd, B.M. Cohen, P.F. Renshaw, Choline, myo-inositol, and mood in bipolar disorder: a proton magnetic resonance spectroscopic imaging study of the anterior cingulate cortex, Bipolar. Disord. 2 (2000) 207–216.

[54] M.J. Berridge, C.P. Downes, M.R. Hanley, Neural and developmental actions of lithium: a unifying hypothesis, Cell 59 (1989) 411–419.

[55] B.W. Agranoff, S.K. Fisher, Inositol, lithium, and the brain, Psychopharmacol. Bull. 35 (2001) 5–18.

[56] S. Avissar, G. Schrieber, A. Danon, R.H. Belmaker, Lithium inhibits adrenergic and cholinergic increases in GTP binding in rat cortex, Nature 331 (1988) 440–442.

[57] M. Roux, M. Bloom, Ca^{2+}, Mg^{2+}, Li^+, Na^+, and K^+ distributions in the headgroup region of binary membranes of phosphatidyl choline and phosphatidylserine as seen by deuterium NMR, Biochemistry 29 (1990) 7077–7089.